

# Spreading of thermonuclear flames on the neutron star in SAX J1808.4–3658: an observational tool

Sudip Bhattacharyya<sup>1,2</sup>, and Tod E. Strohmayer<sup>2</sup>

## ABSTRACT

We analyse archival Rossi X-Ray Timing Explorer (RXTE) proportional counter array (PCA) data of thermonuclear X-ray bursts from the 2002 outburst of the accreting millisecond pulsar SAX J1808.4–3658. We present evidence of nonmonotonic variations of oscillation frequency during burst rise, and correlations among the time evolution of the oscillation frequency, amplitude, and the inferred burning region area. We also discuss that the amplitude and burning region area evolutions are consistent with thermonuclear flame spreading on the neutron star surface. Based on this discussion, we infer that for the 2002 Oct. 15 thermonuclear burst, the ignition likely occurred in the mid-latitudes, the burning region took  $\sim 0.2$  s to nearly encircle the equatorial region of the neutron star, and after that the lower amplitude oscillation originated from the remaining asymmetry of the burning front in the same hemisphere where the burst ignited. Our observational findings and theoretical discussion indicate that studies of the evolution of burst oscillation properties during burst rise can provide a powerful tool to understand thermonuclear flame spreading on neutron star surfaces under extreme physical conditions.

*Subject headings:* equation of state — methods: data analysis — stars: neutron — X-rays: binaries — X-rays: bursts — X-rays: individual (SAX J1808.4–3658)

## 1. Introduction

X-ray bursts are produced by thermonuclear burning of matter accumulated on the surfaces of accreting neutron stars (Woosley, & Taam 1976; Lamb, & Lamb 1978). During many bursts, millisecond period brightness oscillations are generated by the combination

---

<sup>1</sup>Department of Astronomy, University of Maryland at College Park, College Park, MD 20742-2421

<sup>2</sup>X-ray Astrophysics Lab, Exploration of the Universe Division, NASA's Goddard Space Flight Center, Greenbelt, MD 20771; sudip@milkyway.gsfc.nasa.gov, stroh@clarence.gsfc.nasa.gov

of rapid stellar rotation and an asymmetric brightness pattern on the neutron star surface (Strohmayer, & Bildsten 2003). The period of these oscillations is very close to the stellar spin period (Chakrabarty et al. 2003; Strohmayer et al. 2003). Moreover, as this timing feature originates from the surface of the neutron star, its detailed modeling may be useful to constrain stellar structure parameters, and hence the equation of state models of the dense matter in the neutron star core (Bhattacharyya et al. 2005; Miller, & Lamb 1998; Nath, Strohmayer, & Swank 2002; Muno, Özel, & Chakrabarty 2002).

Modeling of burst oscillations can also be useful to understand neutron star atmospheres, surface fluid motions, and for mapping the magnetic field structure on the stellar surface. For example, the evolution of frequency of these oscillations during the burst rise phase, may provide information on the spreading of thermonuclear flames under the extreme physical conditions that exist on neutron stars (e.g., Bhattacharyya & Strohmayer 2005). This is because bursts almost certainly ignite at a particular point on the stellar surface (as simultaneous ignition over the whole surface would require very fine tuning), and then spread to burn all the surface fuel (Fryxell & Woosley 1982; Cumming & Bildsten 2000; Spitkovsky, Levin, & Ushomirsky 2002; Bhattacharyya & Strohmayer 2006a). This slow (compared to the rotational speed) movement and spreading of the burning region (along with other physical effects such as the increased scale height due to burning) may give rise to complex frequency evolution of the observed burst oscillations. This spreading would also cause the observed burst intensity to increase, and the oscillation amplitude to decrease. Moreover, the increase in emission area can be estimated by spectral analysis (Strohmayer, Zhang & Swank 1997; Bhattacharyya & Strohmayer 2006a; 2006b). Therefore, simultaneous modeling of the evolution of burst intensity, oscillation frequency and amplitude, and spectral properties can, in principle, be a powerful tool to understand the propagation of burning fronts on neutron star surfaces under conditions of extreme radiative pressure, magnetic field and gravity.

Frequency evolution during burst rise oscillations has so far been observed from two low mass X-ray binary (LMXB) systems: SAX J1808.4–3658 and 4U 1636–536 (Chakrabarty et al. 2003; Bhattacharyya & Strohmayer 2005). The Rossi X-ray Timing Explorer (RXTE) observed the 401 Hz X-ray pulsar SAX J1808.4–3658 in October and November of 2002, when it was in outburst. Four type I X-ray bursts were detected during these observations (Chakrabarty et al. 2003), three of which showed strong millisecond period brightness oscillations during burst rise. A previous study found that as the burst intensity rises, the oscillation frequency also increases by  $\sim 5$  Hz and may overshoot the stellar spin frequency (Chakrabarty et al. 2003). Here, we analyse these archival data in order to model the time evolution of different burst properties and search for correlations among them.

In our study we find evidence of nonmonotonic variations in the oscillation frequency

during the rising phase of bursts. This is the first report of such variations from any source. The frequency modulation is correlated with the evolution of oscillation amplitude and burning region area. In § 3, we discuss that the correlated amplitude and area evolution is consistent with thermonuclear flame propagation on the neutron star surface.

## 2. Data Analysis and Results

We analyse the archival RXTE proportional counter array (PCA) data of the 2002 outburst from SAX J1808.4–3658. Three thermonuclear bursts with significant millisecond oscillations during the rising phase are found in the ObsIds: 70080-01-01-000 (Oct 15), 70080-01-02-000 (Oct 18), and 70080-01-02-04 (Oct 19). First we explore the frequency evolution of burst rise oscillations during these bursts using three procedures. We calculate dynamic power spectra (Strohmayer & Markwardt 1999) with time sampling short enough to resolve the burst rise interval, but large enough to accumulate sufficient signal power above the noise level. The dynamic spectra (panel *a* of Fig. 1, and Fig. 2) provide indications of the frequency evolution behavior. To confirm the indications in the dynamic spectra, we carry out a phase timing analysis (Muno et al. 2000). We divide the burst rise time interval into several bins of a fixed chosen length, and then assuming a frequency evolution model, we calculate the average phase ( $\psi_k$ ) in each bin ( $k$ ). The corresponding  $\chi^2$  is calculated using the formula  $\chi^2 = \sum_{k=1}^M (\psi_k - \bar{\psi}_k)^2 / \sigma_{\psi_k}^2$  (Strohmayer & Markwardt 2002), where  $M$  is the number of bins. For this study we used extensive burst rise simulations to evaluate the uncertainty,  $\sigma_{\psi_k}$ , as a function of the  $Z^2$  power in each time bin. We find the best fit parameter values for various frequency evolution models by minimizing  $\chi^2$ , and we calculate the uncertainty in each parameter by finding the change which produces the appropriate increase in  $\chi^2$  (Strohmayer & Markwardt 2002; Press et al. 1992). Finally, we calculate the total  $Z^2$  power (Strohmayer & Markwardt 2002) for the entire rise interval (ie. without binning) using the best fit frequency evolution model parameters, and ensure that this power is close to the maximum power obtained from any parameter values.

We first fit the oscillations during the rising phase of the Oct. 15 burst with a constant frequency model. This gives a best fit frequency of 400.91 Hz and  $\chi^2/\text{dof} = 30.04/8$ . We evaluate the significance of this  $\chi^2$  value using simulations, and find a probability of 0.005 to obtain such a value by chance. Since the constant frequency model does not describe the data well, we next consider more complex models. These are; (1) linear frequency increase, (2) second order polynomial, and (3) linear increase and subsequent linear decrease models (see Table 1 for a description of the models). These models give  $\chi^2/\text{dof}$  values of 17.73/7, 17.35/6, and 11.68/5 respectively. Although these models give better fits, they still have

reduced  $\chi^2$  values  $> 2$ , and do not describe the data very well. A slightly more complex model which fits the data well has a linear frequency increase followed by a second order polynomial, and gives a  $\chi^2/\text{dof}$  value of  $3.36/4$ . Of the models tested we consider this the best description of the Oct. 15 burst, and the best fit parameter values are given in Table 1. Panel *a* of Fig. 1 shows that this model is consistent with the dynamic power contours, and it indicates a frequency increase (by a few Hertz) for the first  $\sim 0.2$  s from burst onset, then a frequency decrease (by  $\sim 1$  Hz), and a subsequent increase. From Table 1, we note that the model parameters  $\nu_0$  &  $\dot{\nu}_1$  are practically unconstrained from the lower and upper sides respectively. This implies that the initial frequency increase can be well fit by a very steep model. However, the other sides of these parameters are reasonably well constrained, which shows that a constant frequency model is insufficient to model this portion. Next we fit the rise oscillations from the Oct. 18 & Oct. 19 bursts with the same frequency evolution models. The constant frequency model for the Oct. 18 burst gives a  $\chi^2/\text{dof} = 154.51/8$ , and hence can be strongly rejected. This confirms the conclusions of Chakrabarty et al. (2003) who first noted the large frequency increase present during this burst. A linear frequency increase model gives a  $\chi^2/\text{dof} = 19.35/7$  that, though better, is still uncomfortably large to be acceptable. The next more complex model (a constant frequency, & subsequent linear increase) gives a  $\chi^2/\text{dof} = 8.44/6$  (see Table 1, and the upper panel of Fig. 2), and is statistically acceptable. However, we note that the dynamic power contours (upper panel, Fig. 2) are suggestive of an initial frequency increase, decrease, and increase behavior (shown by the dotted curve) qualitatively similar to that for the Oct. 15 burst. Although higher signal to noise ratios per time bin would likely be required to confirm this behavior, this (dotted curve) model does give a higher total  $Z^2$  power than that given by the best fit  $\chi^2$  model (solid curve) in Table 1. Finally, the constant frequency model for the Oct. 19 burst gives a  $\chi^2/\text{dof} = 22.03/8$ , which is also unacceptably high. A linear frequency increase model (see Table 1, and the lower panel of Fig. 2) gives a  $\chi^2/\text{dof} = 6.46/7$ , and is acceptable for this burst. We note that although the oscillation frequency behavior of the Oct. 19 burst is different from that of the Oct. 15 & 18 bursts, the former burst seems otherwise similar to the latter ones. For example, all three bursts show photospheric radius expansion, and their rise times and durations are  $\leq 1$  s and a few tens of seconds respectively. Thus, the variations in inferred frequency evolution must be associated with some variable which does not drastically alter the gross properties of the burst. One possible variable might be the initial latitude of ignition, although large variations in this quantity might be expected to affect other burst properties, such as the rise time, as well. Panel *b* of Fig. 1 shows the rms amplitude variation with time during the rise of the Oct. 15 burst. From the beginning of the burst, the amplitude decreases for  $\sim 0.2$  s, and then assumes a near constant value, with some fluctuations. This behavior is qualitatively similar to that seen in bursts from the LMXB systems 4U 1728-34 and 4U 1636–536 (Strohmayer, Zhang & Swank 1997; Bhattacharyya &

Strohmayer 2005). We also perform time resolved spectral fitting (using a blackbody model) during the rise of the Oct. 15 burst. The inferred source radius (which provides some relative indication of the size of the burning region on the stellar surface) shows evidence for a modest increase for the first  $\sim 0.2$  s, and then remains almost constant (panel *c*, Fig. 1). Panel *d* gives the corresponding source temperature variation.

### 3. Discussion

Taken together our results for the three bursts from SAX J1808.4–3658 suggest that the oscillation frequency can evolve in a complex manner during burst rise. In all cases a constant frequency model is a poor description of the oscillations. In two bursts (Oct. 15 and 18) the data can best be described by a complex modulation in frequency whereby it initially increases, then decreases before increasing again. Moreover, the oscillation amplitude and the inferred burning region area are found to be correlated with the frequency. We now discuss from a theoretical perspective how spreading of thermonuclear flames can plausibly account for these observations. In our discussions we use the observational results mostly from the Oct. 15 burst as characteristic. The salient features of this burst are as follows: (1) from the start of the burst, the oscillation frequency and burning region area increase and the oscillation amplitude decreases for  $\sim 0.2$  s; (2) after  $\sim 0.2$  s, the frequency first decreases and then increases, and both amplitude and burning region area reach a nearly constant value (with some fluctuations).

The burst begins when the fuel (i.e., accumulated matter) ignites at a particular point, and then the flame propagates over the surface (Fryxell & Woosley 1982; Spitkovsky et al. 2002; Bhattacharyya & Strohmayer 2006a; 2006b). Before spreading has engulfed the entire star, temperature variations due to surface waves may not be able to explain the brightness oscillation or its frequency evolution (as has been proposed for the burst tail oscillations; Heyl 2005; Lee & Strohmayer 2005), as the rapid spreading and temperature increase may wash out this effect. This explanation of oscillations during burst rise was also shown to be unfavored by Bhattacharyya & Strohmayer (2005). However, thermonuclear burning in a limited portion (hot spot) of the neutron star surface can give rise to these oscillations, and the propagation of the burning front may explain the observed time evolution of oscillation properties.

In order to understand how thermonuclear flame spreading can give rise to the observed evolution of oscillation amplitude and burning region area, we first review some relevant results from previous work (Spitkovsky et al. 2002): (1) the greater scale height of the burning region than the cold fuel gives rise to a shearing speed (as the horizontal pressure

gradient in the burning front increases with height). As a result, the cold fuel is drawn into the burning front and ignited. This enables the burning front to propagate. (2) The shearing speed is greater nearer the equator than the pole (due to the latitude dependence of the Coriolis parameter; Spitkovsky et al. 2002). Thus, the burning front propagates with the shearing speed ( $v$ ) (assuming the mixing time scale is very small; Spitkovsky et al. 2002; Fujimoto 1988; Cumming & Bildsten 2000). Now, if the fuel ignites at a mid-latitude (say, in the northern hemisphere), it will propagate faster towards the equator (than the pole), and the east-west width of the burning region will increase much faster near the equator. Therefore, after a certain time, the burning region will encircle the equator and propagate more or less symmetrically towards the south pole. The northern burning front propagates towards the north pole, keeping the asymmetry (due to the variation of east-west width with latitude; see Figure 8 of Spitkovsky et al. 2002), which vanishes near the pole. At the beginning, the burning region is relatively small, and hence the oscillation amplitude can be large. As the burning region grows, the oscillation amplitude naturally diminishes (Fig. 1). This effect was also reported for bursts from other sources (Strohmayer, Zhang, & Swank 1997). After the burning region encircles the equator with a considerable north-south width, the observed burning area does not increase much (hence the near constant radius after the initial increase; see Fig. 1). From this time, the oscillation is due to the residual asymmetry of the northern burning front (with the persistent background due to the azimuthally symmetric portion of the burning region), and hence the amplitude attains a near constant value till the asymmetry vanishes. Therefore, according to our explanation, for the Oct. 15 burst, the burning region takes  $\sim 0.2$  s to nearly encircle the stellar equator. However, we note that this explanation does not include the effects of magnetic field, which may affect the burning front propagation considerably (see below).

Thermonuclear flame propagation may give rise to the observed frequency evolution, if the eastbound and the westbound burning fronts have different accelerations, causing acceleration (either eastwards or westwards) of the center of the burning region relative to the star. Now considering this picture of the azimuthal shift of the hot spot center, an observed oscillation frequency lower than the stellar spin frequency may be caused by the westward motion of the burning region center (for an eastward rotating star). An increased scale height in this region may cause such motion, because, as the hot portion of the burning region puffs up, its top portion slips westwards to conserve angular momentum. If the shearing speed due to this is  $v$ , the center of the burning region moves westward with a speed  $v$  relative to the stellar surface. However, this effect alone can not explain an oscillation frequency that is more than  $\sim 2$  Hz lower than the stellar spin frequency (Cumming & Bildsten 2000). Therefore, as the initial oscillation frequency of the Oct. 15 burst is  $\sim 3 - 4$  Hz less than the neutron star spin frequency, this physical effect can only partially explain the initial

frequency of this burst. Moreover, the increased scale height effect can not explain the following observed features: (1) initial quick increase of frequency (as the scale height does not decrease during the beginning of burst rise), (2) oscillation frequency overshooting the stellar spin frequency, and (3) a decrease and subsequent increase of oscillation frequency during the later stage of the burst rise. A physical effect of variable magnitude, that can move the center of the expanding burning region (hot spot) both eastwards and westwards, is required to explain these aspects. This effect can add to the increased scale height effect at the burst onset (if moving the hot spot center westwards), and can compete with the scale height effect to produce the other observed features of frequency evolution (if moving the hot spot center eastwards). At present, such an effect is not known, but the surface magnetic field may be a promising candidate. This is because the surface magnetic field may have its strength amplified and its geometry modified by differential rotation during the flame spreading. This may enhance the magnetic force, which can subsequently modify the shearing flows, and hence can influence the propagation of the burning front (e.g., Cumming et al. 2002). The exact nature and magnitude of this influence will depend on the geometry and the strength of the field. This effect may be particularly important for SAX J1808.4–3658, as this source is a pulsar (and hence probably has a higher magnetic field than non-pulsars), and because the oscillation frequency overshooting the neutron star spin frequency has been observed only from this source. This source also seems different from other sources in other properties such as the quick and large increase of oscillation frequency during burst rise. However, we note that the uniqueness of SAX J1808.4–3658 in terms of burst rise oscillation frequency evolution is not yet well proven, as so far only seven bursts with significant frequency evolution during the rising phase have been observed (three from this source, and four from 4U 1636–536; Bhattacharyya & Strohmayer 2005). Nevertheless, detailed numerical simulations of thermonuclear flame spreading (including magnetic field effects) may be able to explain the observed correlated evolution of oscillation properties during burst rise, and may provide important information about how the flame speed and other flame spreading properties can be influenced by stellar spin, compactness, magnetic field and burst strength. Therefore, we emphasize that burst rise oscillations provide a potentially powerful tool to understand thermonuclear flame spreading on neutron star surfaces under extreme physical conditions.

## REFERENCES

- Bhattacharyya, S., & Strohmayer, T. E. 2005, ApJ, 634, L157.
- Bhattacharyya, S., & Strohmayer, T. E. 2006a, ApJ, 636, L121.
- Bhattacharyya, S., & Strohmayer, T. E. 2006b, ApJ, in press.
- Bhattacharyya, S., Strohmayer, T. E., Miller, M. C. & Markwardt, C. B. 2005, ApJ, 619, 483.
- Chakrabarty, D. et al. 2003, Nature, 424, 42.
- Cumming, A., & Bildsten, L. 2000, ApJ, 544, 453.
- Cumming, A., Morsink, S. M., Bildsten, L., Friedman, J. L., & Holz, D. E. 2002, 564, 343.
- Fujimoto, M. Y. 1988, A&A, 198, 163.
- Fryxell, B. A., & Woosley, S. E. 1982, ApJ, 261, 332.
- Heyl, J. S. 2005, MNRAS, 361, 504.
- Lamb, D. Q., & Lamb, F. K. 1978, ApJ, 220, 291.
- Lee, U., & Strohmayer, T. E. 2005, MNRAS, 361, 659.
- Miller, M. C. & Lamb, F. K. 1998, ApJ, 499, L37.
- Muno, M. P., Fox, D. W., Morgan, E. H. & Bildsten, L. 2000, ApJ, 542, 1016.
- Muno, M. P., Özel, F., & Chakrabarty, D. 2003, ApJ, 595, 1066.
- Nath, N. R., Strohmayer, T. E. & Swank, J. H. 2002, ApJ, 564, 353.
- Press, W. H., Teukolsky, S. A., Vetterling, W. T., & Flannery, B. P. 1992, Numerical Recipes in FORTRAN (New York: Cambridge University Press), 687-693.
- Spitkovsky, A., Levin, Y. & Ushomirsky, G. 2002, ApJ, 566, 1018.
- Strohmayer, T. E., & Bildsten, L. 2003, in *Compact Stellar X-ray Sources*, Eds. W.H.G. Lewin and M. van der Klis, (Cambridge University Press: Cambridge), (astro-ph/0301544).
- Strohmayer, T. E. & Markwardt, C. B. 1999, ApJ, 516, L81.



Strohmayer, T. E. & Markwardt, C. B. 2002, ApJ, 577, 337.

Strohmayer, T. E., Markwardt, C.B., Swank, J. H., & in 't Zand, J. 2003, ApJ, 596, L67.

Strohmayer, T. E., Zhang, W. & Swank, J. H. 1997, ApJ, 487, L77.

Woosley, S. E., & Taam, R. E. 1976, Nature, 263, 101.

Table 1. Frequency evolution model parameters<sup>a</sup> (with  $1\sigma$  error) for burst rise oscillations of three bursts from SAX J1808.4–3658.

Burst date	$\nu_0$	$\dot{\nu}_1$	$t_{b_1}$	$\dot{\nu}_2$	$\ddot{\nu}_2$	$\chi^2/\text{dof}$	$Z_1^{2b}$
2002 Oct 15	$396.72_{-21.73}^{+2.00}$	$29.64_{-13.95}^{+236.21}$	$0.20_{-0.10}^{+0.05}$	$-15.54_{-4.94}^{+4.73}$	$23.67_{-9.81}^{+11.52}$	3.36/4	152.16
2002 Oct 18	$398.22_{-0.21}^{+0.20}$	–	$0.31_{-0.04}^{+0.04}$	$19.21_{-3.39}^{+5.19}$	–	8.44/6	62.83
2002 Oct 19	$399.64_{-0.14}^{+0.23}$	$1.69_{-0.42}^{+0.07}$	–	–	–	6.46/7	86.64

<sup>a</sup>Frequency evolution model:  $\nu(t) = \nu_0 + \dot{\nu}_1 t$  (for  $t \leq t_{b_1}$ , and  $\nu_0 = \nu(0)$ );  $\nu(t) = \nu(t_{b_1}) + \dot{\nu}_2(t - t_{b_1}) + \ddot{\nu}_2(t - t_{b_1})^2$  (for  $t \geq t_{b_1}$ ).

<sup>b</sup>Fundamental power during burst rise.

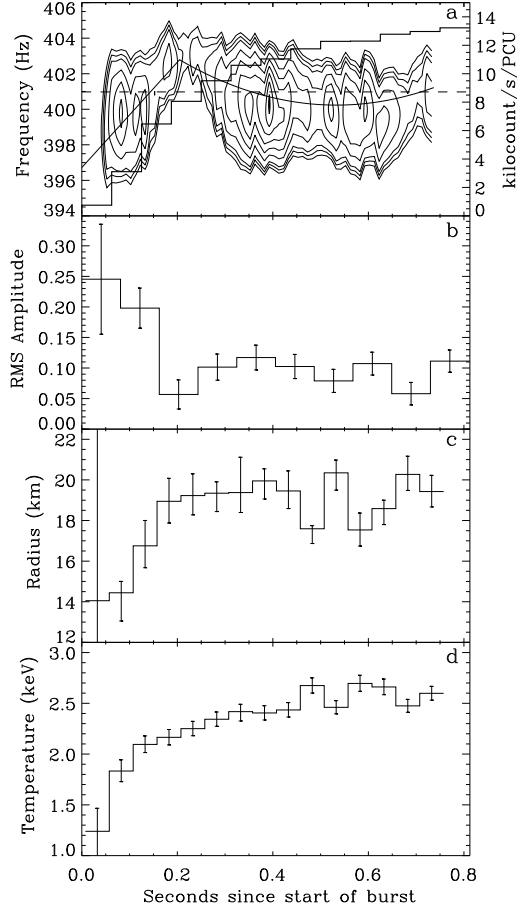


Fig. 1.— Time evolution of different observed burst properties during the rise of the Oct 15 burst from SAX J1808.4–3658. Panel *a* gives the detected intensity (histogram), power contours (minimum and maximum power values are 16 and 51) from the dynamic power spectra (for 0.15 s duration at 0.01 s intervals), the best fit model from Table 1, and the neutron star spin frequency (broken horizontal line). Panel *b* shows the rms amplitude of the oscillations. Here the horizontal lines give the binsize. Panel *c* gives the inferred radius (assuming 10 kpc source distance) of the source, while panel *d* gives the corresponding temperature. For panels *b*, *c*, and *d*, persistent emission is subtracted and a deadtime correction is applied, and the error bars are  $1\sigma$  values.

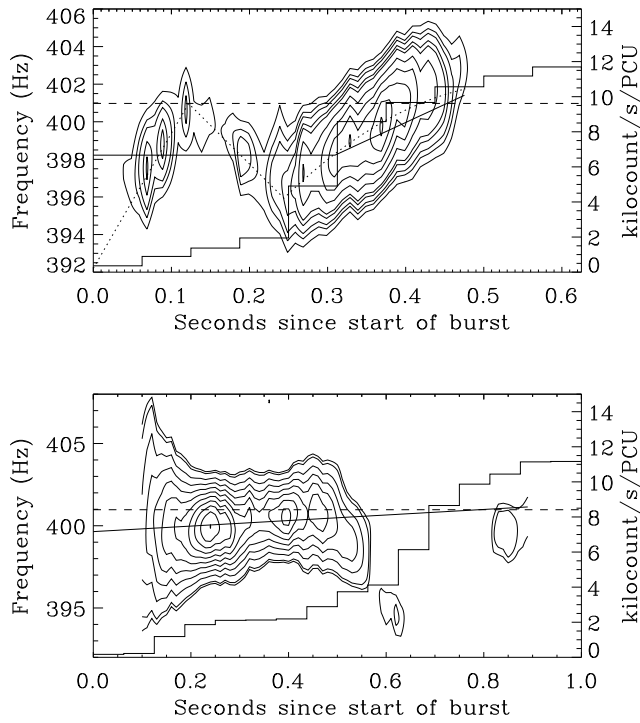


Fig. 2.— Similar to panel *a* of Fig. 1 but for the Oct 18 (upper) and Oct 19 (lower) bursts. For the upper panel dynamic power spectra are calculated for 0.15 s duration at 0.01 s intervals, while for the lower panel these numbers are 0.2 s and 0.01 s. For the calculation of power contours, minimum and maximum power values are 15 and 50 for the upper panel, and 17 and 111 for the lower panel. The dotted line in the upper panel gives the frequency evolution for which the total power (74) is higher than that (63) corresponding to the best fit model (solid line) from Table 1.